Comparison of Two Computationally Feasible Image Deblurring Techniques for Smartphones

C-H. Chang, S. Parthasarthy, and N. Kehtarnavaz
Department of Electrical Engineering, University of Texas at Dallas, Richardson, TX 75080

Abstract— **This paper presents a comparison of two computationally efficient motion deblurring techniques that have been shown to be practically feasible for deployment on smartphones. One technique involves the use of smartphone inertial sensors to provide an estimate of blur causing point-spread-function and the other involves the use of a short-exposure image that is obtained electronically at the same time the blurred image is captured. Both objective and subjective evaluations are carried out for a comprehensive comparison of these two techniques. It is shown that on average the technique utilizing a short-exposure image leads to more effective deblurrring outcomes compared to the technique utilizing inertial sensors.**

Keywords – Computationally efficient image deblurring on smartphones, mobile imaging, computational photography

I. INTRODUCTION

The problem of image deblurring has been extensively examined in the image processing literature and in particular by the computational photography community. Many motion deblurring techniques, e.g. [1-6, 8, 9], attempt to estimate the point-spread-function (PSF) causing the blurring effect. Then, the PSF is used as part of a blind deconvolution procedure to reduce the blur. Much emphasis has been put into algorithms that detect the movements of local image features, such as edges [5] or optical flow [6], for the purpose of estimating the blur causing PSF.

There exist implementation limitations when deblurring solutions are to be deployed on smartphones due to the relatively limited computational and memory resources of such devices. From a practical standpoint, blind deconvolution algorithms are computationally demanding and thus do not run in real-time on smartphones. In addition, it has been shown that ringing artifacts are still visible when using such algorithms. Consider the scenario when an image is taken by a smartphone and the image appears blurred due to handshake motion. The question is considering that the scene of interest or the moment of interest is gone, would it be possible to add an option to the smartphone camera menu to deblur the image in a relatively short amount of time (less than 1 sec) on the smartphone? In [7], we attempted to address this question by electronically (no mechanical part) forming a short-exposure image at the same time an image was taken without requiring any user intervention. The short-exposure image did not suffer from the blurring effect but appeared darker than the original image. Then, the mean and contrast or variance of the blurred image were used to correct the exposure of the short-exposure but unblurred image via tonal correction in an adaptive way. More recently, another computationally efficient approach for deployment on smartphones has appeared in [8] utilizing the inertial measurement units (IMUs) or sensors that exist on smartphones. The IMUs were used to estimate the blur causing PSF due to handshake motion. The low computational complexity of this approach also makes its deployment feasible on smartphone platforms.

In this paper, we provide both an objective and a subjective comparison between the above two techniques that have proven to be suitable for deployment on smartphones due to their low computational complexities. The rest of the paper is organized as follows: Section II presents an overview of these two computationally feasible techniques for smartphones while section III presents our objective and subjective comparison results together with their discussion. Concluding remarks are then stated in section IV.

II. OVERVIEW OF COMPUTATIONALLY FEASIBLE DEBLURRING TECHNIQUES FOR SMARTPHONES

In this section, an overview of the two image deblurring algorithms that have been previously shown to be computationally suitable for smartphone platforms is presented. One algorithm uses IMUs to generate the blur causing PSF and a corresponding deblurred image, and the other uses a short-exposure image to generate a deblurred image via adaptive tonal correction (ATC).

A. Deblurring using IMUs

A blurred image due to handshakes can be modeled by the following equation:

$$\boldsymbol{B} = \boldsymbol{I} \otimes \boldsymbol{G} + \boldsymbol{N} \tag{1}$$

where $\otimes$ denotes the convolution operation, $\boldsymbol{I}$ the original image, $\boldsymbol{G}$ the blur causing PSF and $\boldsymbol{N}$ additive noise.

These days smartphones are equipped with 6-DOF IMU sensors. These sensors were used in [8] to estimate the acceleration and angular velocity associated with handshake motions. The smartphone camera movement trajectory in 3D coordinates $[x,y,z]$ was mapped to 2D coordinates through the reprojection relation $\boldsymbol{P}$ as expressed by Equation (2) [9]

$$\boldsymbol{P}([\boldsymbol{x},\boldsymbol{y},\boldsymbol{z}]^T) = [\frac{\boldsymbol{xf}}{\boldsymbol{z}},\frac{\boldsymbol{yf}}{\boldsymbol{z}}]^T , \tag{2}$$

where f denotes the focal length of the smartphone camera, and z represents the object distance. By assuming the depth is spatially-invariant during the exposure time period τ, the PSF $G(\tau)$ can be written as follows:

$$G(\tau) = \frac{f}{z}\begin{bmatrix} \phi_x(\tau) \\ \phi_y(\tau) \end{bmatrix} \quad (3)$$

where $\phi_x(\tau)$ and $\phi_y(\tau)$ denote 2D position vectors along the x and y direction, respectively. The calculation of the position vectors $\phi_x(\tau)$ and $\phi_y(\tau)$ is achieved by the integration of the acceleration along the x and y directions. As a result, $G(\tau)$ can be viewed as the camera movement in 2D coordinates which is then used to reduce the blur via Wiener filtering. In the implementation of this deblurring technique, the IMU data is recorded by the smartphone inertial sensor during an image capture. Then, the IMU data is processed to obtain an estimate of the PSF. Fig. 1 shows an example PSF found in this manner together with a handshake blurred image and the corresponding deblurred image.

B. *Deblurring using Adaptive Tonal Correction*

In this technique, as reported in [7], a shorter duration of the exposure time (normally one-third) is used to form a short-exposure image at the same time an image is captured. This is achieved by electronically shortening the exposure time without using any mechanical component. In most cases, the blurring effect does not appear in the short-exposure image, while this image appears darker looking. The ATC algorithm adjusts the parameters of two tonal correction curves so that when the short-exposure image is passed through them, it would end up having more or less the same mean and contrast as the blurred but original exposure image. In this technique, the computation of the blur causing PSF is avoided.

The following tonal curve equation was used in [7]:

$$h(u) = \frac{\log(\alpha u - u + 1)}{\log \alpha} \quad (6)$$

where u denotes the input pixel value, and α is a control parameter for changing the tonal curve shape. In Equation (6), the parameter value α is selected such that the brightness level in the short-exposure image is made close to the brightness level of the original exposure image which appears blurred due to handshake motion. A second tonal correction curve is also applied to adjust the contrast in a similar fashion by using the following tonal correction curve:

$$g(u) = \frac{\tan^{-1}(\beta(h(u) - 0.5) + 0.5)}{2\tan(\frac{\beta}{2})} \quad (7)$$

where the parameter value β is selected such that the contrast of the short-exposure image is made close to the contrast of the blurred image. A binary search is used to find α and β in a computationally efficient manner. In [7], α was varied from 1 to 20 in 1.0 step size increments and β was varied from 1 to 5 in 0.3 step size increments. An example of a blurred image, the corresponding short-exposure image, and the deblurred image are shown in Fig. 2.

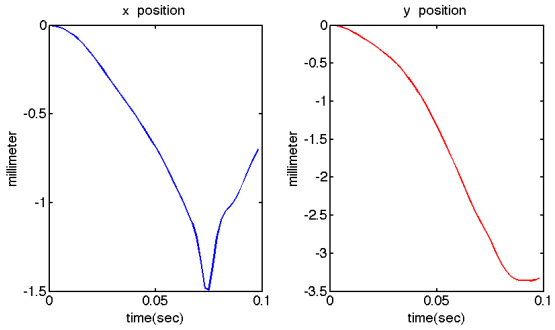

(a) x and y camera translation positions

(b) blur causing PSF

(c) original image (d) deblurred image

Figure 1. Deblurring using IMU technique: (a) translation positions, (b) blur causing PSF, (c) original image appearing blurred due to handshake motion, and (d) deblurred image

III. Objective and Subjective Comparisom Results and Disscussion

In this section, the objective and subjective comparison results between the above two techniques are provided. First, a database was put together by capturing 50 image sets under different lighting and background conditions and with different handshake motions. We used the auto-bracketing approach when collecting the image sets in order to have references images for deblurred images. Each image set consisted of three images that were taken with three different exposure settings. First image was taken with no handshake motion to provide the reference image. The second image was captured by using a shorter exposure time setting to provide

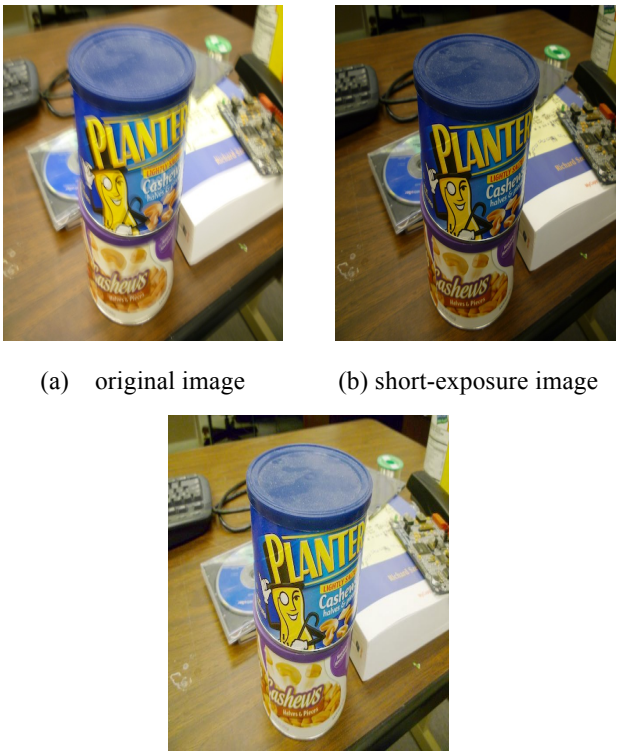

(a) original image (b) short-exposure image

(c) deblurred image

Figure 2. Deblurring using ATC technique: (a) original image appearing blurred due to handshake motion, (b) short-exposure image, and (c) deblurred image

the short-exposure image. The third image was taken by intentionally generating handshakes and by using the normal exposure time setting. Fig. 3 illustrates a sample of the deblurred images based on the above two techniques together with the reference image. These images can be viewed at https://sites.google.com/site/imagedeblurring13/.

A. *Objective comparison*

To evaluate the performance in an objective manner, the performance metrics of structural similarity index measure (SSIM) and mean squared error (MSE) [10,11] were computed. These two metrics are widely used in assessing objective image quality. The SSIM and MSE metrics were calculated based on the reference images, the PSF deblurred images, and the ATC deblurred images.

Figs. 4 and 5 show the objective comparison results corresponding to MSE and SSIM, respectively. As can be seen from these figures, consistently over the 50 image sets examined, the ATC technique outperformed the PSF technique. On average, the MSE for the PSF technique was approximately 1.5 higher compared with the MSE for the ATC technique. On average, the SSIM for the PSF technique was 0.45 and for the ATC technique was 0.7 indicating a closer structural match to the reference images.

B. *Subjective comparison*

In our subjective comparison, 10 viewers were asked to visually inspect the deblurred images in a blind fashion without knowing which image belonged to which technique. Each viewer was asked to decide the better deblurred image or if necessary equally vote for both. Fig. 6 shows the outcome of our subjective comparison. As illustrated in this figure, on average, 96% of the viewers selected the ATC deblurring, and 4% selected the PSF deblurring using IMU. No cases received equal voting by the viewers. This subjective comparison outcome was found consistent with the objective comparison results.

IV. Conclusion

Two practically or computationally feasible image deblurring techniques for smartphones have been examined and compared in this paper. One technique utilizes the IMUs in smartphones to generate a deblurred image from a captured image that appears blurred due to handshake motion and one technique utilizes adaptive tonal correction to generate a deblurred image. By examining 50 image sets under different lighting conditions and backgrounds, it was found that the adaptive tonal correction technique provided more effective deblurred images in terms of both objective and subjective measures.

References

[1] R. Fergus, B. Singh, A. Hertzmann, S. Roweis and W. Freeman, "Removing camera shake from a single photograph," *ACM Trans. Graph*, vol. 25, pp. 787-794, 2006.

[2] T. Portz, L. Zhang, and H. Jiang "High-quality video denoising for motion-based exposure control," *Proceedings of IEEE International Conference on Computer Vision Workshop*, pp. 9-16, 2011.

[3] M. Ben-Ezra and S. Nayar, "Motion-based motion deblurring," *IEEE Trans. on Pattern Analysis and Machine Intell.*, vol. 6, no. 26, pp. 689-698, 2004.

[4] M. Trimeche, D. Paliy, M. Vehvilainen, V. Katkovnik "Multichannel image deblurring of raw color component," *Proceedings of SPIE*, vol. 5674, pp. 169-178, 2005.

[5] N. Joshi, R. Szeliski, and D. Kriegman "PSF estimation using sharp edge prediction", *Proceedings of IEEE Conference on CVPR*, pp. 1-8, 2008.

[6] T. Portz, L. Zhang, and H. Jiang "Optical flow in the presence of spatially-varying motion blur," *Proceedings of IEEE Conference on CVPR*, pp. 1752-1759, 2012.

[7] Q. Razligh and N Kehtarnavaz, "Image blur reduction for cell-phone cameras via adaptive tonal correction," *Proceedings of IEEE International Conference on Image Processing*, vol.1, pp. 113-116, 2007.

[8] O. Šindelář and F. Šroubek, "Image deblurring in smartphone device using built-in inertial measurement sensors," *Journal of Electronic Imaging*, vol. 22, issue 1, 2013.

[9] N. Joshi., S. Kang., C. Zitnick and R. Szeliski "Image deblurring using inertial measurement sensors," *ACM SIGGRAPH*, vol. 29, pp. 1-9, 2010.

[10] A. Hore, and D. Ziou, "Image quality Metrics: PSNR v.s SSIM," *Proceedings of IEEE International Conference on Pattern Recognition*, pp. 2366-2369, 2010.

[11] Z. Wang, A. Bovik, H. Sheikh, E. Simoncelli "Image quality assessment from error visibility to structural similarity," *IEEE Trans. on Image Processing*, vol. 13, no. 4, pp. 600-612, 2004.

(a) reference image captured with no handshake motion

(b) image captured with handshake motion

(c) short-exposure image

(d) ATC deblurred image

(e) PSF deblurred image

Figure 3. A sample image set and the corresponding deblurred images using the two techniques of ATC and PSF

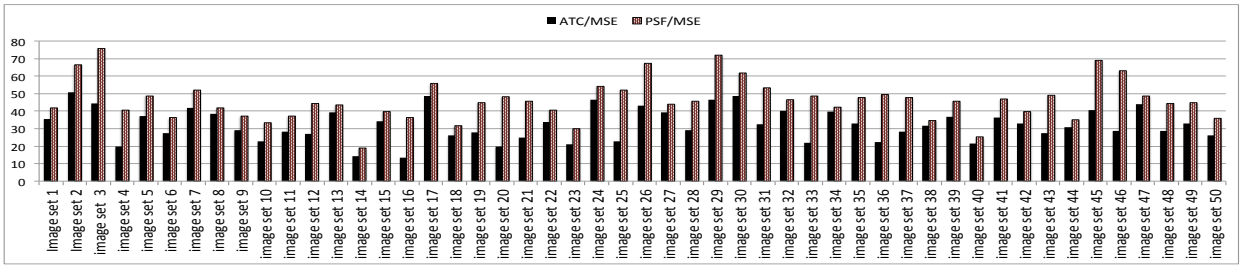

Figure 4. Objective comparison results using MSE

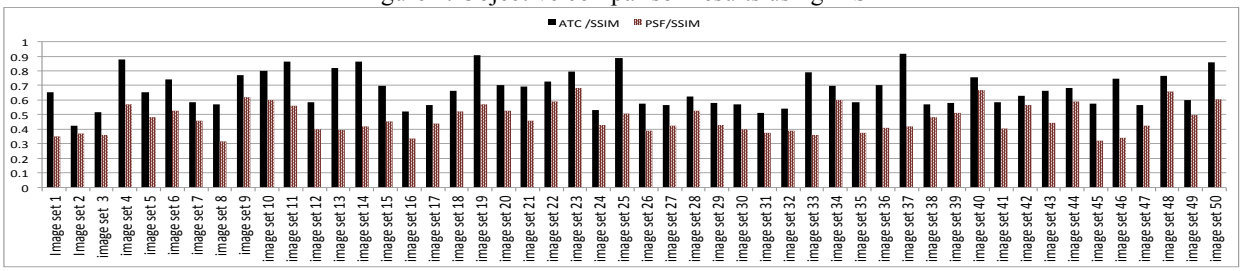

Figure 5. Objective comparison results using SSIM

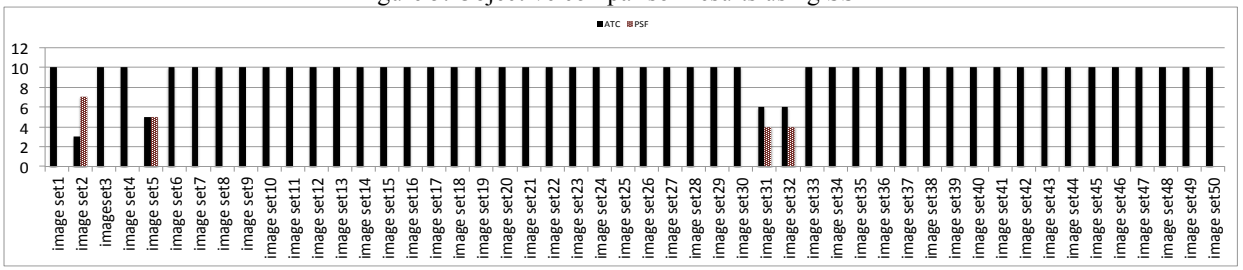

Figure 6. Subjective comparison results